

## Characterization of intermittent lag synchronization

S. Boccaletti<sup>1</sup> and D. L. Valladares<sup>1,2</sup>

<sup>1</sup>*Department of Physics and Applied Mathematics, Universidad de Navarra, Irunlarrea s/n, 31080 Pamplona, Spain*

<sup>2</sup>*Department of Physics, Universidad Nacional de San Luis, Argentina*

(Received 22 November 1999; revised manuscript received 10 February 2000)

Intermittent lag synchronization of two nonidentical symmetrically coupled Rössler systems is investigated. This phenomenon can be seen as a process wherein the intermittent bursts away from the lag synchronization regime correspond to jumps of the system toward other lag configurations. During these jumps, the chaotic trajectory visits closely a periodic orbit. The identification of the different lag configurations and the measure of the fraction of time passed by the system in each one of them provide information on the global scenario of transitions undergone by the system before reaching perfect lag synchronization.

PACS number(s): 05.45.Xt, 05.45.Jn

Synchronization of coupled chaotic oscillators is a field of growing interest. In this framework, four types of synchronization have been studied so far, namely complete synchronization (CS) [1], phase synchronization (PS) [2], and lag synchronization (LS) [3], and generalized synchronization (GS) [4].

CS refers to a process whereby the interaction of two chaotic systems leads to a perfect linking of their chaotic trajectories, so as they remain in step with each other in the course of time. This mechanism was initially proposed to hold for unidirectionally coupled identical systems [1], and later extended to a bidirectional coupling between nonidentical oscillators [3]. GS implies the hooking of the output of one system to a given function of the output of the other system [4]. A symmetric coupling between nonidentical oscillators can lead to an intermediate regime (PS), characterized by a perfect locking of the phases of the two signals, whereas the two chaotic amplitudes remain uncorrelated [2]. Finally, LS consists of hooking one system to the output of the other shifted in time of a lag time  $\tau_{\text{lag}}(s_1(t) = s_2(t - \tau_{\text{lag}}))$  [3].

Experimental verifications of all these theoretical findings have been offered, e.g., in the cardiorespiratory system [5], in the human brain [6], in the cells of paddlefish [7], and in communication with chaotic lasers [8]. Recently, synchronization phenomena have been explored also in high dimensional [9,10] and in space extended chaotic systems [11–15].

In this paper, we focus on the *intermittent lag synchronization* (ILS), a phenomenon recently shown to occur in between PS and LS [3]. We will show that ILS can be characterized in terms of the existence of a set of lag times  $\tau_{\text{lag}}^n$  ( $n=1,2,\dots$ ), such that the system always verifies  $s_1(t) \approx s_2(t - \tau_{\text{lag}}^n)$  for a given  $n$ .

From now on, we will refer to a pair of coupled nonidentical Rössler systems [16], describing the evolution of the three dimensional vectors  $\mathbf{x}_{1,2} \equiv (x_{1,2}, y_{1,2}, z_{1,2})$ :

$$\begin{aligned} \dot{x}_{1,2} &= -\omega_{1,2}y_{1,2} + \varepsilon(x_{2,1} - x_{1,2}), \\ \dot{y}_{1,2} &= \omega_{1,2}x_{1,2} + ay_{1,2}, \\ \dot{z}_{1,2} &= f + z_{1,2}(x_{1,2} - c), \end{aligned} \tag{1}$$

where dots denote temporal derivatives,  $a=0.165$ ,  $f=0.2$ ,  $c=10$  so as Eqs. (1) generate a chaotic dynamics,  $\varepsilon$  represents the coupling strength, and  $\omega_{1,2} \equiv \omega_0 \pm \Delta$  ( $\Delta$  being the frequency mismatch between the two chaotic oscillators). In what follows we focus our study on the case  $\omega_0=0.97$ ,  $\Delta=0.02$ . As  $\varepsilon$  increases, [3] identifies subsequent transitions in system (1) from no synchronization to PS, to LS, and to CS, and traces each one of these transitions in the Liapunov spectrum. In particular, in the range  $0.11 < \varepsilon < 0.14$  (that is in between perfect PS and perfect LS), [3] describes the occurrence of ILS, that is a situation where most of the time the system verifies  $|x_2(t) - x_1(t - \tau_0)| \ll 1$  ( $\tau_0$  being a lag time), but where bursts of local nonsynchronous behavior may occur. In this range of coupling strengths, the typical output of system (1) is reported in Fig. 1. This phenomenon was identified with *on-off* intermittency and the reason for the local excursions from LS was identified in the fact that the second *global* Liapunov exponent of Eq. (1) is negative, but small in absolute value, so the dynamical evolution can drive the system to attractor regions wherein the *local* Liapunov exponent is still positive.

A suitable tool for studying LS is the similarity function  $S(\tau)$ , defined as the time averaged difference between  $x_2(t)$  and  $x_1(t - \tau)$ , conveniently normalized to the geometrical average of the two mean signals

$$S^2(\tau) = \frac{\langle (x_2(t) - x_1(t - \tau))^2 \rangle}{(\langle x_1^2(t) \rangle \langle x_2^2(t) \rangle)^{1/2}}, \tag{2}$$

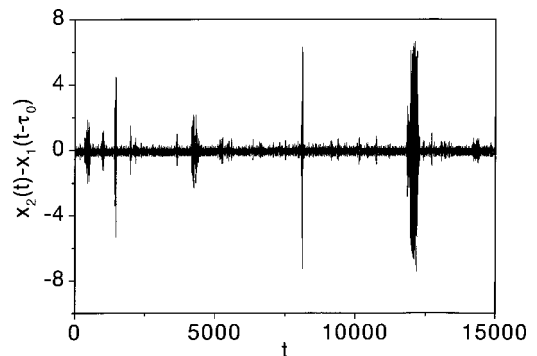


FIG. 1. The time series  $x_2(t) - x_1(t - \tau_0)$  in the ILS regime:  $\varepsilon = 0.13$ ,  $\tau_0 = 0.32$ . Horizontal axis is labeled with time.

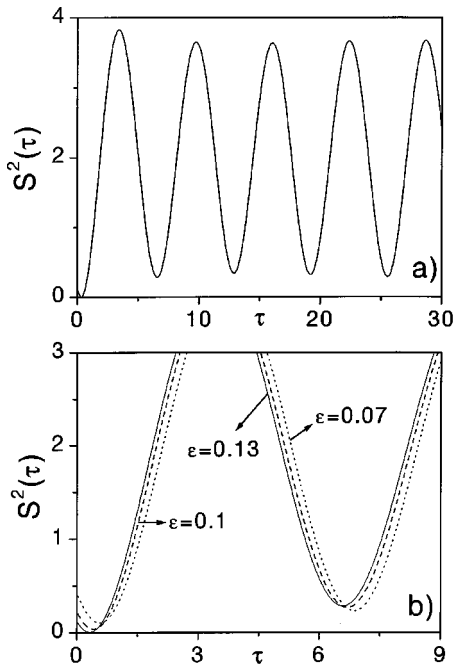


FIG. 2. (a) Similarity function  $S^2(\tau)$  vs the lag time  $\tau$  for  $\varepsilon=0.13$  (intermittent lag synchronization). Notice the presence of a global minimum  $\sigma \approx 0$  at  $\tau_0=0.32$ , and of many local minima for larger lag times  $\tau_n$  ( $n=1,2,3,\dots$ ). (b) Zoom of (a). Solid line:  $\varepsilon=0.13$ , dashed line:  $\varepsilon=0.1$ , dotted line:  $\varepsilon=0.07$ .

where  $\langle \dots \rangle$  denotes temporal average. Indeed, if the similarity function shows a global minimum  $\sigma = \min_{\tau} S(\tau)$ , for  $\tau_0 \neq 0$ , this is an indication of the presence of a principal lag time  $\tau_0$  between the two processes. Notice that Eq. (2) accounts only for linear correlations between the signals  $x_1$  and  $x_2$  and that more complex relations would be required to be investigated by means of nonlinear similarity statistics. However, for our purposes, Eq. (2) provides all the necessary information for the study of LS and ILS.

In Fig. 2(a), we report the similarity function for  $\varepsilon=0.13$ , that is within ILS. Looking at Fig. 2(a), one clearly realizes that, besides a global minimum  $\sigma \approx 0$  at  $\tau_0=0.32$ ,  $S(\tau)$  displays many other local minima at larger lag times  $\tau_n$  ( $n=1,2,3,\dots$ ). These local minima witness that system (1), besides being lag synchronized most of the time with respect to the global minimum  $\tau_0$ , during its dynamical evolution occasionally visits closely other lag configurations corresponding to  $|x_2(t) - x_1(t - \tau_n)| \ll 1$ . The deepness of the  $n$ th local minimum is in close relationship with the fraction of time that the corresponding lag configuration is closely visited by system (1). Even though none of the lag configurations with  $n > 0$  can be considered a lag synchronization regime (only the lag configuration with  $n=0$  can be made stable for a suitable choice of  $\varepsilon$ ), in the following we will show that their study provides an alternative tool to identify the transitions from no synchronization to PS and LS in system (1). Furthermore, the different lag times  $\tau_n$  can be expressed by the relation  $\tau_n = \tau_0 + nT$ ,  $T$  being the return time of system (1) onto its Poincaré section (that is, the reciprocal of the mean peak in the Fourier spectrum). This fact is intimately related to the phase coherence properties of the Rössler system.

Both the location and the deepness of all local minima are

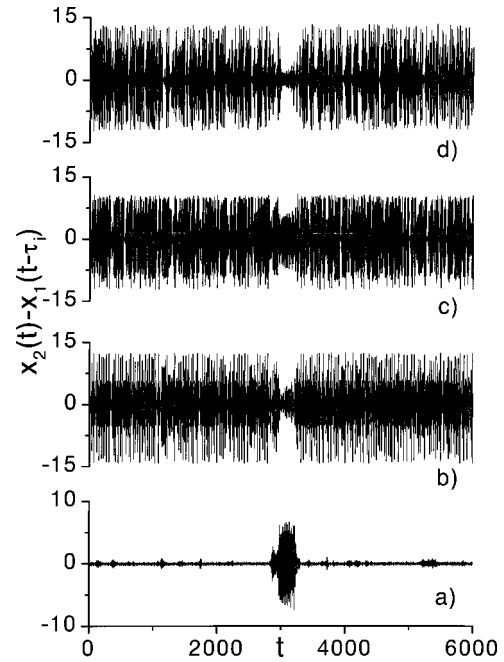


FIG. 3. Temporal behavior of the differences  $\Delta_n = x_2(t) - x_1(t - \tau_n)$ , for  $n=0$  (a),  $n=1$  (b),  $n=2$  (c), and  $n=3$  (d). In all cases  $\varepsilon=0.13$ . (a)  $\tau_0=0.32$ ; (b)  $\tau_1=6.60$ ; (c)  $\tau_2=12.87$ ; (d)  $\tau_3=19.20$ .

functions of the coupling strength  $\varepsilon$ . Figure 2(b) reports a zoom of the similarity function (limited to the first two local minima) at different values of  $\varepsilon$ . As the coupling strength increases, two different phenomena can be observed in Fig. 2(b), namely a drift of all  $\tau_n$  toward the origin, and a change in their corresponding deepness. Precisely, the value of the local minima  $\tau_n$  increases, while the value of the global minimum  $\tau_0$  decreases, vanishing eventually at larger  $\varepsilon$  values. The decreasing process of  $\tau_0$  reveals that, by increasing the coupling strength, the system will eventually lead to a CS state (wherein  $\tau_0$  must vanish). The increasing process of the values of the local minima tells us that one is approaching a perfect LS state [wherein the fraction of time spent by system (1) in the configuration  $|x_2(t) - x_1(t - \tau_0)| \ll 1$  must increase, and consequently the fraction of time spent in all configurations  $|x_2(t) - x_1(t - \tau_n)| \ll 1$ ,  $n \neq 0$  must vanish].

Figure 2 suggests that we look carefully not only to lag synchronization phenomena with respect to the principal lag time  $\tau_0$  (as already reported in [3]), but also to the occurrence of the other lag configurations with  $n > 0$  during ILS. To this purpose, we select  $\varepsilon=0.13$  in system (1) and monitor the differences  $\Delta_n = x_2(t) - x_1(t - \tau_n)$ ,  $n=0,1,2,3$  (for this particular choice of  $\varepsilon$ ,  $\tau_0=0.32$ ,  $\tau_1=6.60$ ,  $\tau_2=12.87$ , and  $\tau_3=19.20$ ). The results are shown in Fig. 3. For most of the time the oscillations of  $\Delta_0$  are strongly bounded. Correspondingly the oscillations of  $\Delta_n$  are very large for all  $n$ . However, during the burst of local nonsynchronous behavior (with respect to the lag time  $\tau_0$ ), the oscillations of  $\Delta_1$  and  $\Delta_3$  range within a limited interval. This means that, during the bursts occurring in ILS, the system visits closely another lag configuration corresponding to some lag time  $\tau_n$ . In other words, one can interpret ILS as the coexistence of many lag configurations (each one of them corresponding to a different local minimum of the similarity function) and the

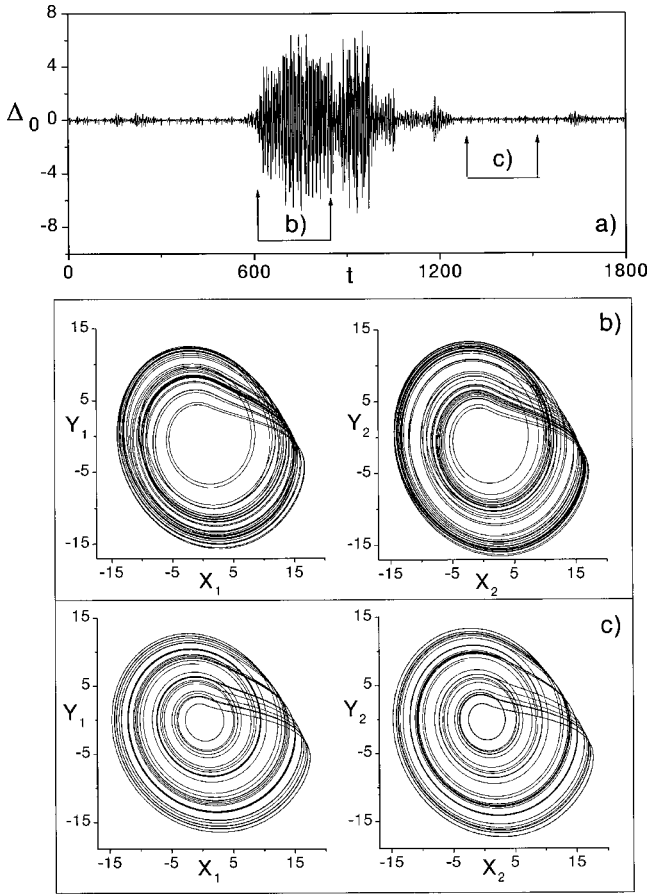


FIG. 4. (a) Temporal evolution of  $\Delta_0$  during the occurrence of an intermittent burst ( $\varepsilon = 0.13$ ). (b) and (c): projections of the portion of the chaotic trajectories of the two systems onto the corresponding  $(x, y)$  planes within (b) and outside (c) the intermittent burst. The considered portions of the dynamical evolution (done by 7500 points, corresponding to about 40 oscillations) are designed with arrows in (a).

intermittency phenomena can be regarded as erratic jumps from one to another of such configurations. The situation may be more complex, including situations where multiple jumps among different  $\tau_n$  lag configurations may occur within the same burst.

In order to better visualize what is happening, we compare the dynamics of system (1) inside and outside the intermittent bursts. In Fig. 4(a) we report a snapshot of the dynamical evolution of  $\Delta_0$  for  $\varepsilon = 0.13$  around the occurrence of an intermittent burst. We then selected two different temporal regions [denoted by arrows in Fig. 4(a)], namely a region inside and one outside the burst. The corresponding portions of the chaotic trajectory of system (1) can be visualized in the subspaces  $(x_1, y_1)$  and  $(x_2, y_2)$  [Fig. 4(b) within the burst, and Fig. 4(c) outside the burst]. The two trajectory portions have been selected so as to contain the same number of oscillations (around 40), in order to qualitatively highlight the relative differences between the two cases. While outside the burst the trajectory is spread within the chaotic attractor [Fig. 4(c)], inside the burst one can clearly appreciate the

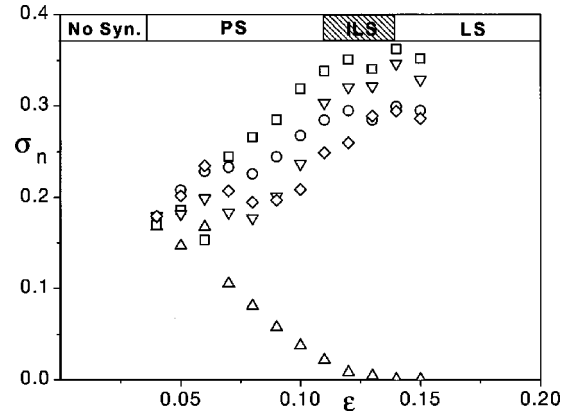


FIG. 5.  $\sigma_n$  (see text for definition) vs the coupling strength  $\varepsilon$  for  $n=0$  (triangles up),  $n=1$  (circles),  $n=2$  (squares),  $n=3$  (triangles down), and  $n=4$  (diamonds). The parameter ranges for PS, ILS, and LS are indicated in the upper part of the figure.

multibranch structure closely visited by the chaotic trajectory, revealing proximity to a period 2 orbit.

Finally, let us discuss how the function (2) can provide a way (alternative with respect to the study of the Liapunov spectrum) for tracing the global scenario of transitions toward synchronized states occurring in system (1). To this purpose we consider the values  $\sigma_n(\varepsilon) \equiv S^2(\tau_n(\varepsilon))$  of the different local minima of  $S^2(\tau)$ , and we report them as functions of  $\varepsilon$  in Fig. 5. While  $\sigma_0$  is a monotonically decreasing function of  $\varepsilon$ , all the other  $\sigma_n$   $n \neq 0$  increase together with the coupling strength. At  $\varepsilon = \varepsilon_{LS} \approx 0.145$ ,  $\sigma_0$  vanishes, thus indicating that the system selects a unique lag time in its synchronous evolution. Therefore  $\varepsilon_{LS}$  can be taken as the transition point for perfect lag synchronization. Another important feature evident from Fig. 5 is that all  $\sigma_n$  converge to the same value at  $\varepsilon = \varepsilon_{PS} \approx 0.036$ . Surprisingly,  $\varepsilon_{PS}$  is the transition point for system (1) from a nonsynchronized state toward perfect phase synchronization. Both PS and ILS regimes are characterized by a nonzero  $\sigma_0$  and by different values of  $\sigma_n$   $n \neq 0$ , thus reflecting the coexistence of many lag configurations.

The values of  $\varepsilon_{PS}$  and  $\varepsilon_{LS}$  extracted in Fig. 5 coincide with the transition points individuated in [3] by studying the variations of the Liapunov spectrum. More precisely,  $\varepsilon_{PS}$  coincides with the point where one of the zero Liapunov exponents in the spectrum becomes negative, and  $\varepsilon_{LS}$  with the point where the second positive Liapunov exponent becomes negative. The conclusion is that the study of the similarity function and of the behavior of its local minima provides an alternative way to trace the subsequent transitions in system (1) toward synchronized states.

The authors are indebted to C. Grebogi, J. Kurths, Y. C. Lai, and M. G. Rosenblum for many fruitful discussions. Work partly supported by Ministerio de Educacion y Ciencia, Spain (Grant No. PB95-0578), Universidad de Navarra, Spain (PIUNA). S.B. acknowledges financial support from EU Contract No. ERBFMBICT983466. D.L.V. acknowledges financial support from an AECI grant.

- [1] L.M. Pecora and T.L. Carroll, Phys. Rev. Lett. **64**, 821 (1990).
- [2] M.G. Rosenblum, A.S. Pikovsky, and J. Kurths, Phys. Rev. Lett. **76**, 1804 (1996).
- [3] M.G. Rosenblum, A.S. Pikovsky, and J. Kurths, Phys. Rev. Lett. **78**, 4193 (1997).
- [4] N.F. Rulkov, M.M. Sushchik, L.S. Tsimring, and H.D.I. Abarbanel, Phys. Rev. E **51**, 980 (1995); L. Kocarev and U. Parlitz, Phys. Rev. Lett. **76**, 1816 (1996).
- [5] C. Schafer, M.G. Rosenblum, J. Kurths, and H.H. Abel, Nature (London) **392**, 239 (1998).
- [6] P. Tass, M.G. Rosenblum, M.G. Weule, J. Kurths, A. Pikovsky, J. Volkman, A. Schnitzler, and H.J. Freund, Phys. Rev. Lett. **81**, 3291 (1998).
- [7] A. Neiman, X. Pei, D. Russell, W. Wojtenek, L. Wilkens, F. Moss, H.A. Braun, M.T. Huber, and K. Voigt, Phys. Rev. Lett. **82**, 660 (1999).
- [8] G.D. Van Wiggeren and R. Roy, Science **279**, 1198 (1998).
- [9] K. Pyragas, Phys. Rev. E **58**, 3067 (1998).
- [10] M.J. Bünner, and W. Just, Phys. Rev. E **58**, R4072 (1998).
- [11] A. Pikovsky, M.G. Rosenblum, and J. Kurths, Europhys. Lett. **34**, 165 (1996).
- [12] P. Parmananda, Phys. Rev. E **56**, 1595 (1997).
- [13] A. Amengual, E. Hernández-García, R. Montagne, and M. San Miguel, Phys. Rev. Lett. **78**, 4379 (1997).
- [14] S. Boccaletti, J. Bragard, F.T. Arecchi, and H.L. Mancini, Phys. Rev. Lett. **83**, 536 (1999).
- [15] H. Chaté, A. Pikovsky, and O. Rudzick, Physica D **131**, 17 (1999).
- [16] O.E. Rössler, Phys. Lett. **57A**, 397 (1976).